Geochimica et Cosmochimica Acta, Vol. 69, No. 5, pp. 1359–1369, 2005

0016-7037/05 $30.00 + .00

doi:10.1016/j.gca.2004.08.023

Negative $\delta^{18}O$ values in Allan Hills 84001 carbonate: Possible evidence for water precipitation on Mars

G. Holland,* J. M. Saxton, I. C. Lyon, and G. Turner

School of Earth, Atmospheric, and Environmental Sciences, University of Manchester, Manchester M13 9PL, UK

(*Received January* 28, 2004; *accepted in revised form August* 25, 2004)

Abstract—The Martian meteorite ALH84001 contains ~1% by weight of carbonate formed by secondary processes on the Martian surface or in the shallow subsurface. The major form of this carbonate is chemically and isotopically zoned rosettes which have been well documented elsewhere. This study concentrates upon carbonate regions ~200 μm across which possess previously unobserved magnesium rich inner cores, interpreted here as rosette fragments, surrounded by a later stage cement containing rare Ca-rich carbonates (up to $Ca_{81}Mg_{07}Fe_{04}Mn_{07}$) intimately associated with feldspar. High spatial resolution ion probe analyses of Ca-rich carbonate surrounding rosette fragments have $\delta^{18}O_{V\text{-}SMOW}$ values as low as −10‰. These values are not compatible with deposition from a global Martian atmosphere invoked to explain ALH84001 rosettes. The range of $\delta^{18}O$ values are also incompatible with a fluid that has equilibrated with the Martian crust at high temperature or from remobilisation of carbonate of rosette isotopic composition. At Martian atmospheric temperatures, the small CO_2(gas)-CO_2(ice) fractionation makes meteoric CO_2 an unlikely source for −10‰ carbonates. In contrast, closed system Rayleigh fractionation of H_2O can generate $\delta^{18}O_{H2O}$ −30‰, as observed at high latitudes on Earth. We suggest that atmospheric transport and precipitation of H_2O in a similar fashion to that on Earth provides a source of suitably ^{18}O depleted water for generation of carbonate with $\delta^{18}O_{V\text{-}SMOW} = -10‰$.

1. INTRODUCTION

The Martian meteorite ALH84001 has been the subject of intense study following the discovery that it is a unique sample of 4.5Ga Martian crust (Nyquist et al., 1995) and the claims that it contains possible evidence of fossilised Martian life within secondary carbonates (McKay et al., 1996). ALH84001 contains several different carbonate textures (Mittlefehldt, 1994) which can be classified into fine grained, crystalline, partially aligned carbonates described as 'granular bands' (Treiman, 1995), elliptical clasts of carbonate and strongly chemically and isotopically zoned globules, referred to here as carbonate rosettes.

One aspect of ALH84001 petrology that has remained controversial is the formation mechanism of these carbonates. For this reason, there is very little agreement concerning the formation temperature: estimates varying between 0 and 600°C. Precipitation from a relatively low temperature aqueous fluid is favoured by most authors (e.g., Treiman, 1998) on the basis that higher temperatures would remove the observed micron scale chemical and isotopic zoning. This low temperature origin is supported by an estimate of <200°C from cation diffusion modelling (Kent et al., 2001) and <150°C from experimental formation of carbonate globules similar to rosettes (Golden et al., 2000). A low temperature evaporitic origin has been suggested by Harvey and McSween (1998) and Warren (1998) to explain the absence of abundant hydrated phases that would be expected from percolating aqueous fluids. Tentative identification of preterrestrial K-bearing mica in ALH84001 carbonates (Brearley, 1998, 2000) may also provide a useful constraint on formation temperature: an absence of mica lattice intergrowths implies a deposition temperature > 150°C ± 50°C while the absence of muscovite mica implies a deposition temperature < 250°C ± 50°C. In contrast, Scott et al. (1997, 1998) infer rapid crystallisation of carbonate at high temperature from shocked-melted carbonate and Harvey and McSween (1996) invoked carbonate geo-thermometry to infer a high temperature (650°C) origin with carbonates forming from impact-related metasomatism by CO_2 rich fluids. Equilibrium thermodynamics are also cited by Mittlefehldt (1994) as evidence of a high temperature (700°C) hydrothermal fluid origin.

Early oxygen isotope ratio measurements by acid dissolution (Romanek et al., 1994; Jull et al., 1995) yielded bulk values of $\delta^{18}O_{V\text{-}SMOW} = +19‰$ and $\delta^{18}O_{V\text{-}SMOW} = +15 \pm 5‰$ respectively, which was cited as evidence for low temperature formation. High spatial resolution ion microprobe analyses of carbonate rosettes measured isotopic zoning from $\delta^{18}O_{V\text{-}SMOW} = +9.5 \pm 1.1‰$ to $\delta^{18}O_{V\text{-}SMOW} = +20.6 \pm 1.3‰$ (Valley et al., 1997), $\delta^{18}O_{V\text{-}SMOW} = +8 \pm 2.0‰$ to $\delta^{18}O_{V\text{-}SMOW} = +22 \pm 2.0‰$ (Saxton et al., 1998) and $\delta^{18}O_{V\text{-}SMOW} = +5.4 \pm 0.8‰$ to $\delta^{18}O_{V\text{-}SMOW} = +25.3 \pm 0.8‰$ (Leshin et al., 1998) from core to rim respectively. The correlation of carbonate chemistry with the isotopic zoning present in zoned ALH84001 carbonate globules (e.g., Leshin et al., 1998; Saxton et al., 1998) indicates that the isotopic zonation is directly related to the progress of carbonate crystallisation and can therefore be used to derive quantitative constraints on formation conditions and parameters. In addition, Saxton et al. (1998) and Eiler et al. (2002) measured a $\delta^{18}O_{V\text{-}SMOW}$ value of ~0‰ for ankeritic ALH84001 carbonate. The textural relationship between this ankerite and carbonate rosettes is unclear. The present study extends the work of Saxton et al., (1998) to areas of Ca-rich carbonate (up to ~80 molar% Ca).

In this paper we present major element and oxygen isotope

* Author to whom correspondence should be addressed (g.holland@manchester.ac.uk).

data of carbonate with a view to testing the validity of previous models and we attempt to explain both the environment of carbonate deposition and the origin of the source fluids.

2. ANALYTICAL PROCEDURE

2.1. Samples

We studied 3 small (2–5 mg) grains of ALH84001 from subsample ALH84001,287. These chips were mounted in epoxy and polished to expose carbonate on flat surfaces. Optical inspection after polishing revealed regions of carbonate ~200 μm^2 which occurred at the edges of these grains in all three cases. This may be expected as the grains would break most easily along carbonate fractures that could also have acted as fluid conduits, resulting in carbonate deposition.

2.2. Chemical Analyses

Preliminary scanning electron microscopy studies of selected grains were conducted using the JEOL JSM 6400 Analytical SEM at Manchester. This instrument was used for both imaging in Back Scattered Electron (BSE) mode and quantitative analysis in secondary electron mode using energy dispersive spectrometry (EDS). BSE images were obtained to locate rosettes, employing the high contrast between the dark grey of lower average atomic mass magnesium rich rims and the light grey of the higher average atomic mass calcium/iron rich cores. An accelerating voltage of 15 kV, a beam current of 1.5 nA and a working distance of 39 mm were used when obtaining images.

Chemical analyses of carbonates presented in Electronic Annex EA-1 (Table EA-1) were acquired using the Manchester Cameca SX100 electron microprobe. Quantitative spot analyses were obtained with a spatial resolution of ~1 μm using wavelength dispersive spectrometry (WDS) for Fe, Mn, Ca, Mg and Si, and EDS for other elements with an accelerating voltage of 15 kV and a beam current of 10 to 20 nA. A total of 75 quantitative analyses were made using the SX100 electron microprobe before ion probe analyses (Table EA-3) and 100 SEM analyses after ion probe analysis to further constrain the average composition of the ion probe craters. Fe, Mg, Ca, and Mn element maps with a spatial resolution of ~1 μm were obtained for two carbonate regions using the SX100 although excitation regions for these carbonates vary from 1.7 to 2.55 μm depending on cation chemistry. Fe, Mg, Ca and Si were obtained for the third region. EPMA data were also used to calibrate element maps giving an estimated accuracy of be better than 5%. All element maps are presented in Electronic Annex EA-1.

2.3. Isotopic Analyses

Oxygen isotope data of the carbonate regions were obtained using the Manchester VG Isolab 54 ion microprobe (Saxton et al., 1996) and the University of California, Los Angeles (UCLA) Cameca IMS 1270 ion microprobe. Locations of ion probe spot analyses are shown on the SEM Figures 1a, 2a and 3a.

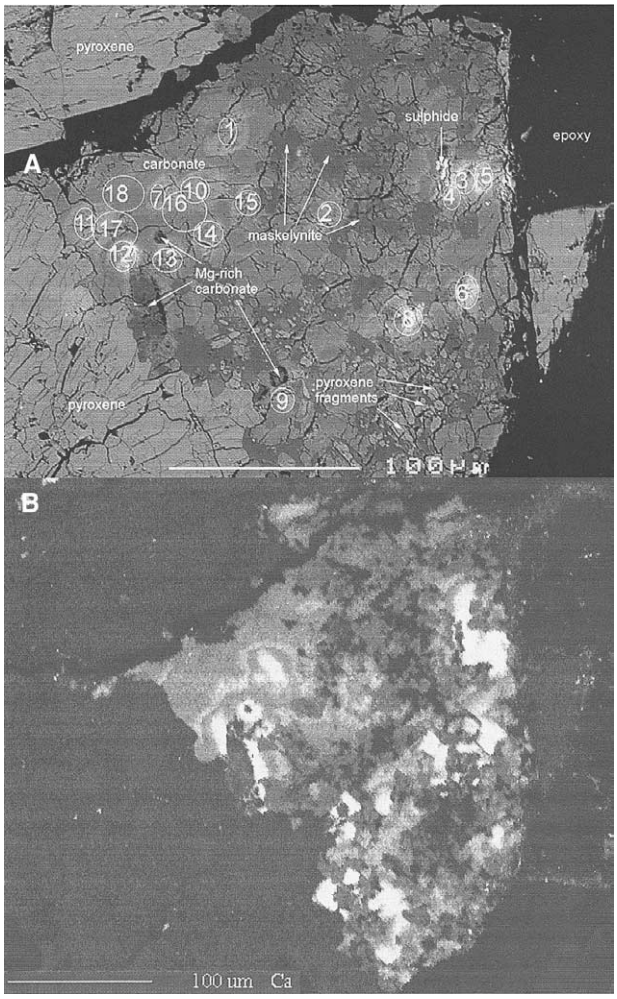

Fig. 1. (a) Back scattered electron image of sample ALH84001, 287a showing interspersed later stage carbonate cement (labelled carbonate) and maskelynite. Numbered ovals are ion microprobe spots (see Table 1). (b) Electron microprobe Ca element map of sample 287a showing Mg-rich carbonate encapsulated in later cement of Ca-rich carbonate.

2.3.1. Manchester

A Cs^+ primary beam with a current of ~0.07 nA and an accelerating voltage of 10 kV (total 18 keV on the sample) was used to sputter the polished sample producing a crater ~10 μm in diameter and up to 1 to 2 μm deep. Low energy (0–22 eV) secondary ions were admitted to a double focusing mass spectrometer allowing simultaneous measurement of ^{16}O, ^{17}O and ^{18}O using a Faraday collector for ^{16}O and conversion dynode systems (CDS) detectors for ^{17}O and ^{18}O (Saxton et al., 1996). Typical count rates for ^{18}O were 50,000 cps. Each measurement comprised 120-s sputter time followed by a 30-s spot measurement time repeated 20 times during each analysis, giving a total ~3×10^7 counts of ^{18}O. Charge compensation was achieved using an 18-kV electron gun to deliver up to 1 μA of electrons to a ~100 by ~300 μm spot on the sample. Twenty-three oxygen isotope spot analyses were made using the Manchester ion microprobe.

The Manchester Isolab 54 ion probe has demonstrated ex-

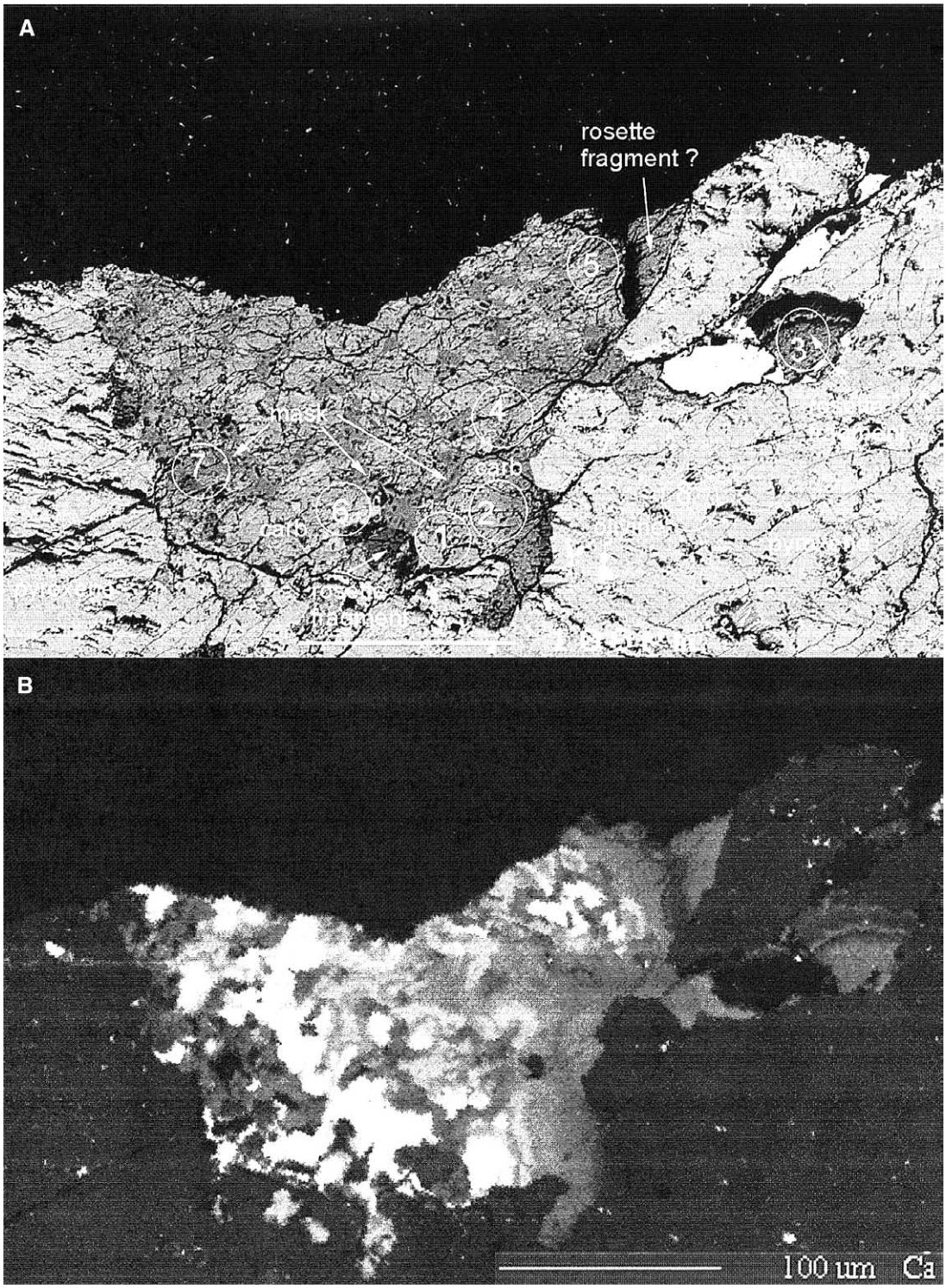

Fig. 2. (a) Back scattered electron image of sample ALH84001, 287b. showing interspersed later stage carbonate cement (carb) and maskelynite (mask). Classic rosette fragment is centre right showing clear differences with 'rosette fragment?' (b) Ca element map of sample 287b showing Mg-rich carbonate encapsulated in Ca-rich carbonate.

ceptional stability in detector gain and instrumental isotopic fractionation over long periods of time (e.g., Saxton et al., 1996, 2000; Jones et al., 2000) with raw (as measured, uncorrected or normalised to any other standard) $^{18}O/^{16}O$ ratios obtained from an ankerite standard showing a 1σ scatter of 2‰ over periods of upto several months. Measurements of samples were nevertheless interspersed with measurements upon standards and we are therefore confident that calibrations for in-

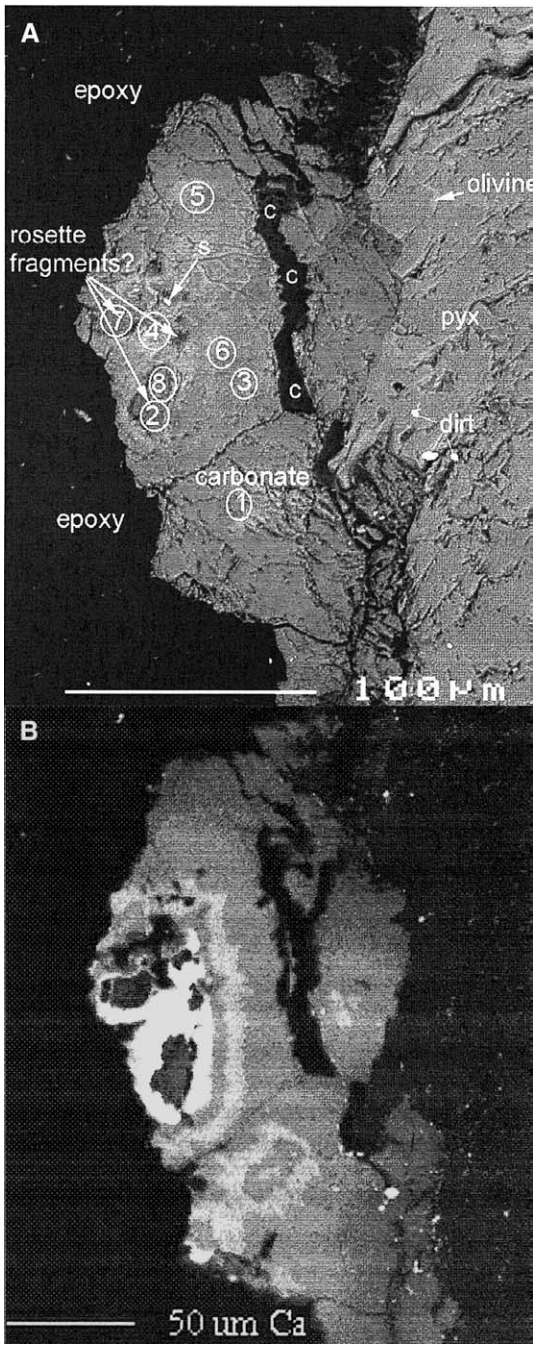

Fig. 3. (a) Back scattered electron image of sample ALH84001, 287c showing texture of Mg-rich carbonate fragments Region labelled 'c' is crack formed during sample preparation; 's' is minor sulphide. 'Dirt' is dust incorporated onto the carbon coating of the polished section before SEM analysis. (b) Ca element map of sample 287c.

strumental fractionation and matrix corrections remained valid over the whole of this data acquisition period.

2.3.2. UCLA

An additional nine analyses were conducted on the UCLA ion microprobe using an ~1-nA Cs^+ primary beam current to generate low energy secondary ions, resulting in a larger spot size (~25 μm diameter) than that of the Manchester ion microprobe. A normal incidence electron flood gun provided charge neutralisation. High primary beam currents provided typical count rates of $\sim 5 \times 10^5$cps of ^{18}O allowing simultaneous measurement of $^{16}O^-$ and $^{18}O^-$ ions in Faraday cups to give precision of ~0.1‰. Each measurement comprised a 120-s sputter time before analysis followed by 10 blocks of 10 s of measurements giving a total $\sim 5 \times 10^7$ counts of ^{18}O. Background counts were measured after every three or four analyses and typical background counts were $<$ 10,000 counts per second of ^{16}O. A Si^- ion image was taken before analysis to minimise contamination of carbonate areas with pyroxene or maskelynite. In this way it is estimated that at worst there is $<$ 5% contamination by oxygen from silicates.

2.3.3. Matrix effects

A major source of isotopic fractionation arises from variability in ionization probability with chemical composition of the sample (known as the 'matrix effect'). This can lead to measured differences in $^{18}O/^{16}O$ ratio of up to 20‰ between minerals of very different chemical composition but the same isotopic composition. This is unacceptable when accuracies of 1 to 2‰ are required. Variation in surface chemical composition, impurities and oxidation state compound this problem. In an attempt to eliminate these effects when analyzing for oxygen we analysed standards of pure calcite, pure magnesite, pure siderite, ankerite of composition $Ca_{51}Mg_{22}Fe_{25}Mn_{02}$ and dolomite of composition $Ca_{50}Mg_{39}Fe_{10}Mn_{00}$. The matrix effects of Martian carbonate of intermediate compositions are then inferred from the end member effects. All standard data are reproduced in Electronic Annex EA-2.

3. RESULTS

3.1. Petrography

Owing to the large number of element maps and the similarities of carbonate morphology in all 3 sections, the element maps and more detailed petrographic description is available in Electronic Annex EA-1. To illustrate textural and chemical variation, SEM images and Ca element maps only are included and the petrography is described here only briefly.

Two of the carbonate regions (287a and 287b) contain feldspathic glass intimately associated with carbonate throughout the 200 μm^2 carbonate-feldspar region (Figs. 1 and 2). The third carbonate region (287c) does not contain feldspathic glass (Fig. 3). In all three grains, carbonate regions engulf Mg-rich fragments of carbonate which show fine-scale chemical zoning from $Ca_{05}Mg_{69}Fe_{24}Mn_{01}$ to $Ca_{09}Mg_{78}Fe_{12}Mn_{01}$ that is similar to rosette mantles and rims. In addition, 287a contains an Mg-rich fragment which has the distinctive texture of a rosette (Treiman, 1998). Therefore we shall describe them as rosette fragments. These rosette fragments are encapsulated by rare Ca-rich carbonates which have chemical composition of $Ca_{45}Mg_{33}Fe_{15}Mn_{07}$ in 287a, $Ca_{76}Mg_{12}Fe_{05}Mn_{06}$ in 287b and $Ca_{74}Mg_{14}Fe_{12}Mn_{08}$ in 287c at their most calcic. This Ca-rich carbonate adjacent to the rosette fragments grades to carbonate of typical composition $Ca_{15}Mg_{51}Fe_{32}Mn_{02}$ at the carbonate-pyroxene boundaries. In addition, a region of Ca-rich carbonate

Table 1. SIMS carbonate matrix effects for Manchester and UCLA ion microprobes. Positive values indicate ion probe measurements with $\delta^{18}O$ greater than the correct value of standard.

Mineral	Manchester (this work) ($\delta^{18}O$ ‰)	UCLA (this work and Leshin et al., 1998) ($\delta^{18}O$ ‰)
Magnesite	–8.4	–15
Siderite	–7.6	–10
Ankerite	+9.8	–6.8
Dolomite	+7.7	–5.6
Calcite	+10.4	–2

of composition $Ca_{78}Mg_{12}Fe_{05}Mn_{05}$ occurs in the upper portion of 287a (Fig. 1a). We shall refer to all carbonate which is not rosette carbonate as later stage cement. It is the most Ca-rich regions of this later stage cement that possess the exceptionally low $\delta^{18}O$ values.

3.2. Oxygen Isotopic Analyses

3.2.1. Manchester

Ankerite of composition $Ca_{51}Mg_{22}Fe_{25}Mn_{02}$ was used as the day to day standard over the four month period during which isotopic analyses of ALH84001 were performed. We assume the 1σ uncertainty of each ALH84001 carbonate measurement to be equal to the scatter in this ankerite standard over this four month observing period. Forty-five standard analyses were made during this period. The 1σ scatter of the day-to-day ankerite standard was 2.0‰. This includes error induced by varying detector sensitivities, any variation in instrumental fractionation due to retuning and variation due to change in external (lab) temperature. Errors from counting statistics are typically 0.5‰ therefore uncertainty for all ALH84001 measurements is taken to be $\sqrt{(2.0^2 + 0.5^2)}$ which is 2.1‰.

3.2.2. UCLA

Analyses of ALH84001 at UCLA were conducted in March 2001 together with the same dolomite $Ca_{50}Mg_{39}Fe_{10}Mn_{00}$ standard and ankerite $Ca_{51}Mg_{22}Fe_{25}Mn_{02}$ standard as Manchester. Previously determined matrix effects (Leshin et al., 1998) were used for more magnesian carbonate and the above standards were used for Ca-rich (>50% Ca) carbonate. Matrix corrections relative to calcite are presented in Table 1. Thirty-four standard analyses were made during this period. The 1σ scatter of the day-to-day ankerite and dolomite standards was 1.1‰. Errors associated with counting statistics are typically 0.1‰ therefore uncertainty for all ALH84001 measurements is taken to be $\sqrt{(1.1^2 + 0.1^2)}$ which is 1.1‰.

Whilst the whole range of carbonate compositions can generate a 20‰ matrix fractionation effect, importantly we note that the matrix effect between calcite-ankerite-dolomite is < 3‰ for the Manchester ion microprobe and < 5‰ for the UCLA ion microprobe. As the important isotope data are from > 50% Ca carbonate, we have additional confidence in our matrix corrected values.

The measured and corrected $\delta^{18}O$ values are shown in Table 2 and Figure 4 with previously published ALH84001 carbonate $\delta^{18}O$ analyses for comparison. The earlier work by Leshin et al. (1998) and Saxton et al. (1998) had demonstrated a correlation between $\delta^{18}O$ values and magnesium abundance in the rosette carbonate and the new data appears to follow the same trend. However, the chemical zoning of the carbonates is not a continuous trend because the rosette fragments are encapsulated by the most Ca-rich carbonates of the later stage cement. Therefore dramatic variation in cation chemistry is accompanied by large variations in $\delta^{18}O$ values (+20 to +25‰ for the rosette fragments and −10 to 0‰ in the surrounding Ca-rich carbonate only 10 μm apart).

4. DISCUSSION

4.1. Unique ALH84001 Carbonate?

The consensus from previous work on ALH84001 carbonates suggests the presence of three different carbonate textures: fine grained 'granular bands' (Treiman, 1995), elliptical clasts of Mg-rich carbonates (Scott, 1999) and globules or rosettes (e.g., Harvey and McSween, 1996; Treiman and Romanek, 1998). Although these three types of carbonate are distinct, cation chemistry and textural relationships suggest they are all a product of one episode of secondary mineralisation (Treiman, 1998, and references therein). Distinct from these carbonates, Eiler et al. (2002) found relatively homogeneous massive regions of ankeritic carbonate (40–80%Ca) up to 1000 μm across associated with feldspar. This may also have been observed previously by Treiman (1998) and Scott (1999). The relationship between these massive ankeritic carbonate regions and 'rosette type' carbonate was not evident in Eiler et al. (2002). Our textures are broadly similar to those described by Eiler et al. (2002) with three important differences:

1. Ca-rich carbonate of the later stage cement, whilst having the same maximum Ca content as ankeritic carbonate of Eiler et al. (2002), extends to Ca poorer compositions such that the carbonate cement composition at the carbonate-pyroxene interface overlaps with rosette cores on a Ca-Mg-Fe+Mn ternary diagram (Fig. 5).
2. Micron scale chemical zoning of later stage cement, clearly observed in Ca and Mn element maps, was not observed in ankeritic carbonate of Eiler et al. (2002).
3. In contrast to the homogeneous Mg carbonate of Eiler et al. (2002), some of the inner Mg-rich carbonate described here possesses clear chemical zoning similar to that of rosettes.

In addition to the three important petrographical and chemical differences between Eiler et al. (2002) and this work, we find that the oxygen isotope data are significantly different in the Ca-rich (>50% Ca) carbonate (Fig. 4). Key points of this dataset are:

1. Rare Ca-rich regions (up to 80% Ca) have very low $\delta^{18}O_{V\text{-}SMOW}$ down to -10 ± 2‰.
2. Adjacent to the 80% Ca carbonate, the inner Mg-rich regions have a $\delta^{18}O_{V\text{-}SMOW}$ of $\sim+22 \pm 2$‰, identical within error to that of rosette rims (Leshin et al., 1998; Saxton et al., 1998).
3. $\delta^{18}O_{V\text{-}SMOW}$ of relatively Ca-rich regions (>30% Ca) agree with Saxton et al. (1998) but are in disagreement with Leshin et al. (1998) and Eiler et al. (2002).

Table 2. Measured $\delta^{18}O$ values and matrix correction relative to day-to-day ankerite standard. (M) is Manchester ion microprobe analyses, (U) is UCLA ion microprobe analyses. Mask is maskelynite and pyx is pyroxene. Note that any contamination of carbonate with silicate would slightly increase the measured $\delta^{18}O$ values for the more Ca-rich carbonate.

Sample and spot number	Raw $\delta^{18}O$ (‰)	Matrix correction (‰)	$\delta^{18}O_{v\text{-}SMOW}$ (‰)	Average chemical composition
(M) 287a spot 1	8.1	+3.7	11.8	$Ca_{13}Mg_{49}Fe_{37}Mn_{01}$
(M) 287a spot 2	6.7	+2.2	8.9	$Ca_{17}Mg_{47}Fe_{34}Mn_{02}$
(M) 287a spot 3	–0.8	–9.1	–9.9	$Ca_{71}Mg_{14}Fe_{07}Mn_{08}$
(M) 287a spot 4	6.7	–8.7	–2.0	$Ca_{60}Mg_{21}Fe_{12}Mn_{07}$
(M) 287a spot 5	5.7	–8.6	–2.9	$Ca_{55}Mg_{25}Fe_{14}Mn_{06}$
(M) 287a spot 6	4.9	–8.5	–3.6	$Ca_{54}Mg_{28}Fe_{13}Mn_{05}$
(M) 287a spot 7	5.6	–0.9	4.7	$Ca_{26}Mg_{41}Fe_{30}Mn_{03}$
(M) 287a spot 8	5.3	–8.5	–3.2	$Ca_{54}Mg_{27}Fe_{13}Mn_{06}$
(M) 287a spot 9	4.2	+0.7	4.9	$Ca_{21}Mg_{45}Fe_{32}Mn_{02}$
(M) 287a spot 10	7.3	–6.5	0.8	$Ca_{44}Mg_{35}Fe_{16}Mn_{05}$
(M) 287a spot 11	5.8	+2.9	8.7	$Ca_{15}Mg_{46}Fe_{38}Mn_{01}$
(M) 287a spot 12	2.2	–2.2	0.0	$Ca_{30}Mg_{40}Fe_{26}Mn_{04}$
(M) 287a spot 13	7.4	0.0	7.4	$Ca_{23}Mg_{41}Fe_{33}Mn_{03}$
(M) 287a spot 14	3.1	+1.5	4.6	$Ca_{19}Mg_{46}Fe_{33}Mn_{02}$
(M) 287a spot 15	4.3	–0.6	3.7	$Ca_{25}Mg_{40}Fe_{30}Mn_{03}$
(U) 287a spot 16	–4.6	+6.7	2.1	$Ca_{35}Mg_{33}Fe_{26}Mn_{05}$
(U) 287a spot 17	0.2	+8.5	8.7	$Ca_{19}Mg_{46}Fe_{32}Mn_{03}$
(U) 287a spot 18	–3.2	+9.0	5.8	$Ca_{16}Mg_{49}Fe_{32}Mn_{03}$
(U) 287b spot 1	–8.6	+6.7	–1.9	$Ca_{51}Mg_{29}Fe_{13}Mn_{06}$
(U) 287b spot 2	–1.6	+9.5	7.9	$Ca_{14}Mg_{52}Fe_{32}Mn_{02}$
(U) 287b spot 3	3.5	+11.0	14.5	$Ca_{09}Mg_{64}Fe_{24}Mn_{01}$
(U) 287b spot 4	–8.6	+11.0	2.4	$Ca_{13}Mg_{53}Fe_{31}Mn_{02}$
(U) 287b spot 5	1.8	+11.0	12.8	$Ca_{08}Mg_{65}Fe_{24}Mn_{01}$
(U) 287b spot 6	–10.8	+5.2	–5.6	$Ca_{63}Mg_{20}Fe_{10}Mn_{07}$
(U) 287b spot 7 mask	–3.5	—	—	—
(U) 287b spot 8 pyx	–0.8	—	—	—
(M) 287c spot 1	3.6	+0.7	4.3	$Ca_{21}Mg_{45}Fe_{32}Mn_{02}$
(M) 287c spot 2	18.4	+5.8	24.2	$Ca_{07}Mg_{70}Fe_{22}Mn_{01}$
(M) 287c spot 3	11.1	+2.9	14.0	$Ca_{15}Mg_{43}Fe_{40}Mn_{02}$
(M) 287c spot 4	9.2	–9.1	0.1	$Ca_{70}Mg_{14}Fe_{09}Mn_{07}$
(M) 287c spot 5	7.1	+4.7	11.8	$Ca_{10}Mg_{55}Fe_{30}Mn_{01}$
(M) 287c spot 6	9.5	+1.1	10.6	$Ca_{20}Mg_{50}Fe_{28}Mn_{02}$
(M) 287c spot 7	13.7	+6.9	20.6	$Ca_{04}Mg_{67}Fe_{29}Mn_{00}$
(M) 287c spot 8	17.3	+5.5	22.8	$Ca_{08}Mg_{69}Fe_{22}Mn_{00}$

4. Mg-Ca-Fe carbonate terminating at the pyroxene boundary has $\delta^{18}O_{V\text{-}SMOW}$ up to $\sim+14 \pm 2$‰.

Whilst recent work by Corrigan and Harvey (2004) on ALH84001 carbonates shows some textural similarities with our carbonates, a detailed petrographic and chemical comparison is beyond the scope of this paper. Confronted with an ALH84001 carbonate showing new textural relationships to carbonate rosettes, new zoning in chemical composition and exceptionally light $\delta^{18}O$ values, we believe these later stage cements constitute a distinct type of ALH84001 carbonate.

4.2. Application of Previous Models to –10‰ Carbonate

4.2.1. High temperature silicate equilibrium

Oxygen isotopic data can place important constraints on the environment of later stage cement deposition. If temperatures $>$ 600°C are employed in either a prolonged high temperature hydrothermal model or in a shock remobilised model, it is necessary to consider the effects of isotopic equilibration with silicate on bulk carbonate isotopic composition. Orthopyroxene, constituting 95% of ALH84001, has $\delta^{18}O_{V\text{-}SMOW} = +4.6$‰ (Shearer et al., 1999). Using fractionation factors of Chiba et al. (1989) for pyroxene-calcite, formation of carbonate at 500°C in equilibrium with pyroxene of $\delta^{18}O_{V\text{-}SMOW} = +4.6$‰ would yield carbonate of $\delta^{18}O_{V\text{-}SMOW} \sim +8$‰ (or $\delta^{18}O_{V\text{-}SMOW} \sim +6.5$‰ at 700°C). These values are significantly higher than the Ca-rich carbonate with $\delta^{18}O_{V\text{-}SMOW} = -10$‰. An additional constraint is provided by measurements of $\Delta^{17}O$ ($\Delta^{17}O = 0.52\delta^{18}O - \delta^{17}O$) which measures movement away from the terrestrial fractionation line (T.F.L.) (Clayton and Mayeda, 1996) on a three-isotope oxygen plot. Bulk silicate measurements (Franchi et al., 1999) yield consistent values of $\Delta^{17}O = +0.3$‰ relative to bulk terrestrial samples but $\Delta^{17}O$ measurements of water extracted from ALH84001 yielded values of +0.8‰ (Karlsson et al., 1992) relative to the T.F.L. Similarly, measurements of CO_2 from ALH84001 carbonates yield $\Delta^{17}O$ of +0.6 to +0.9‰ relative to T.F.L. (Farquhar et al., 1998). These show that the carbonate and fluids which formed them cannot have been in isotopic equilibrium with the silicates. Although $\Delta^{17}O$ of the later stage cement is unknown, one would expect all $\Delta^{17}O$ excess in the rosettes to have been erased if the later stage cement had formed in a prolonged high temperature environment.

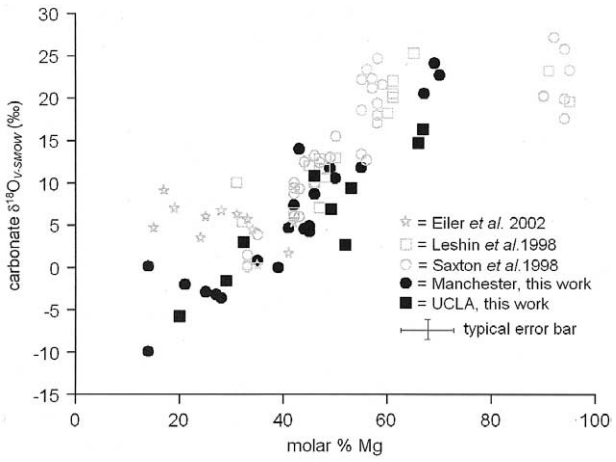

Fig. 4. Isotopic zoning of carbonate with Mg content. Comparison of isotopic data from Leshin et al. (1998) ankerite from Saxton et al. (1998), Eiler et al. (2002), and this work. Error bars (shown once for clarity) are < 5% for chemical composition and 2‰ for $\delta^{18}O$ values.

4.2.2. Closed system models

Eiler et al. (2002) interpreted their ankeritic carbonate to be the product of remobilisation of rosette type carbonate. ALH84001 carbonate observed previously has an average $\delta^{18}O_{V\text{-}SMOW}$ of +15 to +19‰ (Romanek et al., 1994; Jull et al., 1995). If carbonate of this composition is decarbonated during remobilisation, some kinetic isotope fractionation may take place. However, terrestrial examples of shock mobilised and decarbonated calcite indicate that redeposited carbonate is only ~5‰ lower than the preshock carbonate (Martinez et al., 1994). Thus redeposition of carbonate ions will have a bulk $\delta^{18}O_{V\text{-}SMOW}$ of ~+12‰ (a bulk preshock average of +17 − 5‰ due to the shock remobilisation). Even if this lowered bulk value of +12‰ undergoes high temperature (700°C) ankerite-CO_2 fractionation, the carbonate will have a lowest $\delta^{18}O_{V\text{-}SMOW}$ = +6‰ which is significantly higher than $\delta^{18}O_{V\text{-}SMOW}$ −10‰.

Some preliminary work (Skála and Žák, 2001) suggests the isotopic fractionation during shock melting may lower $\delta^{18}O$ of mobilised carbonates by as much as 20‰. If $\delta^{18}O_{V\text{-}SMOW}$ 20‰ fractionation is correct, a bulk carbonate CO_2 value of $\delta^{18}O_{V\text{-}SMOW}$ = −3‰ is generated (+17 − 20‰). A bulk CO_2 value of $\delta^{18}O_{V\text{-}SMOW}$ = −5‰ is required to deposit carbonate with $\delta^{18}O_{V\text{-}SMOW}$ −10‰ at 700°C therefore carbonate with $\delta^{18}O_{V\text{-}SMOW}$ = −10‰ may just be possible. However, a function of the closed system shock model is that the final bulk value must equal that of the starting composition. A bulk value for carbonate of $\delta^{18}O_{V\text{-}SMOW}$ = −3‰ is clearly not compatible with the ion microprobe data showing that the majority of the later stage cement has $\delta^{18}O_{V\text{-}SMOW}$ > 0‰. Also, CO_2 vapour-carbonate fractionation requires that 80% of the cement is precipitated with $\delta^{18}O_{V\text{-}SMOW}$ < 0‰. The samples indicate carbonate with $\delta^{18}O_{V\text{-}SMOW}$ < 0‰ composes < 10% of the later stage cement.

4.2.3. Open system models

Closed system models of carbonate formation do not seem valid for production of carbonate with $\delta^{18}O_{V\text{-}SMOW}$ −10‰. Most authors favour an open system scenario (e.g., Wright et al., 1992; Romanek et al., 1994; Valley et al., 1997; Leshin et al., 1998; Saxton et al., 1998) in which an infinitely large reservoir of H_2O and CO_2 is responsible for carbonate formation. In such an environment, the isotopic composition of the source fluid remains constant as carbonate precipitation proceeds and the $\delta^{18}O$ of the carbonate reflects either a change in the H_2O:CO_2 ratio or a change in temperature. The following two models assume that this reservoir represents the global Martian H_2O and CO_2 values. Using oxygen isotopes we will now explore the possibility that the Ca-rich carbonates of the later stage cement originated from an open system near surface source of H_2O and CO_2 different to the source of rosette carbonates.

The oxygen isotope ratios of CO_2 in the current Martian atmosphere are poorly constrained. Estimates vary from $\delta^{18}O$ = +20 ± 50‰ (Nier and McElroy, 1977) obtained by Viking to $\delta^{18}O$ = −130 ± 80‰ (Krasnopolsky et al., 1996) from Earth based spectroscopy. Therefore we shall follow the initial outgassed high temperature silicate equilibrium model of Clayton and Mayeda (1988). In this model, outgassed fluids with H_2O / (H_2O + CO_2) of 0.8 (hereafter designated X = 0.8) are assumed to have equilibrated at 1000°C with crustal silicate before release to the atmosphere/hydrosphere system. On cooling, the H_2O and CO_2 remain in equilibrium with each other but are isotopically decoupled from the silicate. Clayton and Mayeda (1988) suggested X = 0.8 as it accounted for their measurement of carbonate $\delta^{18}O_{V\text{-}SMOW}$ = +21‰ in EETA79001. Using X = 0.8 yields $\delta^{18}O_{H2O}$ −2.4‰ and $\delta^{18}O_{CO2}$ +43.7‰. These values are just able to generate the complete range of oxygen isotope ratios previously observed in Martian carbonates and are therefore plausible initial values to use in the first instance. This approach was also used by Leshin et al. (1998) to infer 0°C > T_{dep} > 250°C from a wide range of $\delta^{18}O_{V\text{-}SMOW}$ values, where the highest $\delta^{18}O_{V\text{-}SMOW}$ is assumed to have formed at 0°C. Using these assumptions, Saxton et al. (1998) derived core and rim formation temperatures for the carbonate rosettes of 210 and 80°C respectively. A similar approach ($\delta^{18}O_{H2O}$ −5‰ rather than $\delta^{18}O_{H2O}$ −2.4‰) is used by Eiler et al. (2002) to explain ankeritic carbonate with $\delta^{18}O_{V\text{-}SMOW}$ 0‰. If the isotopically heaviest carbonate with $\delta^{18}O_{V\text{-}SMOW}$ = +24‰ forms at the lowest possible temperature of 0°C (unless brines are involved) the H_2O in the source fluid would have a $\delta^{18}O_{V\text{-}SMOW}$ of −12‰ from ankerite-water fractionation (Friedman and O'Neil, 1977). To deposit carbonate with $\delta^{18}O_{V\text{-}SMOW}$ = −10‰ from this fluid requires deposition at > 600°C which, as discussed previously, would remove chemical heterogeneity and induce carbonate-silicate equilibrium resulting in carbonate of $\delta^{18}O_{V\text{-}SMOW}$ = +6‰. It would also remove isotopic heterogeneity observed between the inner Mg-rich region of $\delta^{18}O_{V\text{-}SMOW}$ = +22‰ and the Ca-rich region of $\delta^{18}O_{V\text{-}SMOW}$ = −10‰ over only 10 μm. Therefore using the Clayton and Mayeda (1988) model of 0°C equilibrium temperature for a H_2O-CO_2 fluid after outgassing with X = 0.8 cannot generate −10‰ carbonate. However, if an initial outgassing value of X = 0.5 is used, the $\delta^{18}O_{H2O}$ becomes −15.6‰ and the $\delta^{18}O_{CO2}$ becomes +30.5‰ when the fluid has cooled to 0°C and decoupled from the Martian crust. With this revised value for X, it is possible to precipitate $\delta^{18}O_{V\text{-}SMOW}$ = −10‰ carbonate from a global hydrosphere at relatively low temperatures (<300°C) although as is discussed

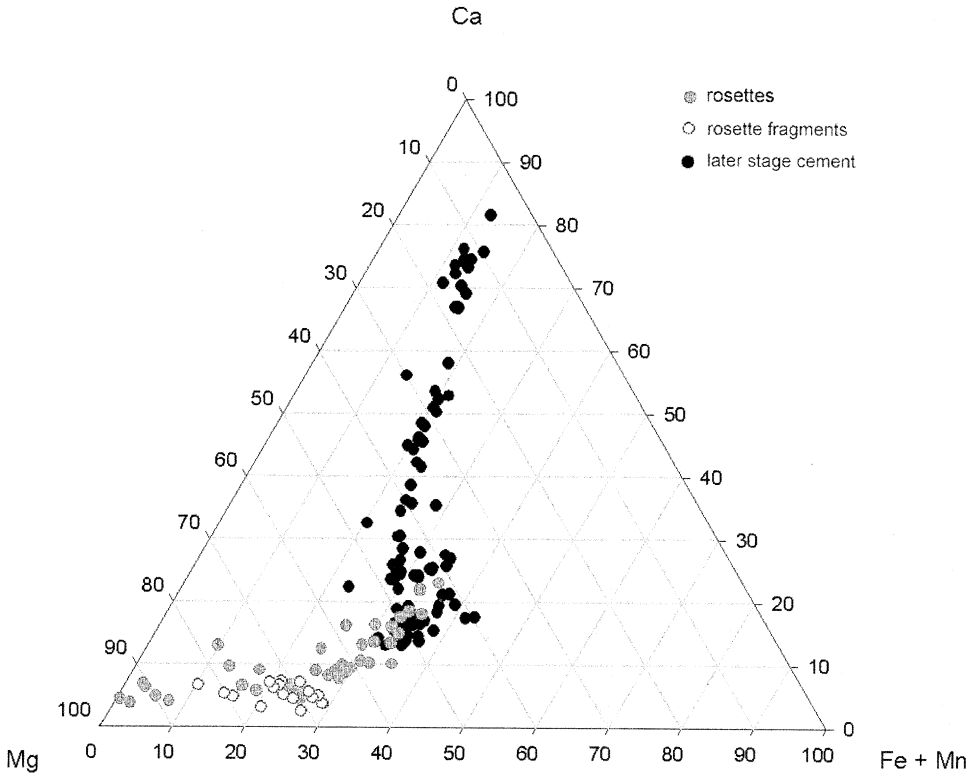

Fig. 5. Cameca SX100 wavelength dispersive spectrometry spot analyses of carbonate from the three ALH84001 samples (errors smaller than data points).

in more detail later, the heaviest carbonates such as those in Nakhla, siderite with $\delta^{18}O_{V\text{-}SMOW} = +34‰$ (Saxton et al., 2000) can no longer be generated from this reservoir.

4.3. New Models

4.3.1. CO_2 dominated environments

The preceding section considered a model by Clayton and Mayeda (1988) invoking high temperature equilibrium of an H_2O-CO_2 fluid ($X = 0.8$) with the surrounding silicate, which then cooled before carbonate deposition. On cooling, oxygen isotope fractionation between H_2O and CO_2 increases, permitting carbonate of between $\delta^{18}O_{V\text{-}SMOW}$ $-2.4‰$ and $+43.7‰$ to precipitate depending on the temperature and ratio of H_2O to CO_2 in this hydrothermal fluid. By changing the initial volatile inventory to $X = 0.5$, the absolute values of the fluid are shifted 18‰ lower to between $\delta^{18}O_{V\text{-}SMOW}$ $-15.6‰$ and $+30.5‰$. (Note the magnitude of the difference between $\delta^{18}O_{CO2}$ and $\delta^{18}O_{H2O}$ is insensitive to initial outgassing estimates.) If we assume a CO_2 dominated environment such as thermal mobilisation of CO_2 ice in the regolith and permit the same process of high temperature silicate equilibrium followed by cooling, oxygen isotope partitioning in the fluid is dominated by CO_2. This prevents the increase in $\delta^{18}O_{CO2}$ which occurs during H_2O controlled CO_2-H_2O equilibrium as the fluid cools ($\delta^{18}O$ difference of ~45‰ at 0°C see above). Using pyroxene-CO_2 fractionation factors of Bottinga and Javoy (1975) between 600 and 900°C, the CO_2 fluid can equilibrate with crustal material (again pyroxene of $\delta^{18}O_{V\text{-}SMOW}$ $+4.6‰$) with very minor fractionation: $\delta^{18}O_{CO2}$ will be between $\delta^{18}O_{V\text{-}SMOW} = +3.5‰$ and $\delta^{18}O_{V\text{-}SMOW} = +5.5‰$ over this temperature range. Putting limited quantities of H_2O in contact with CO_2 yields the range of $\delta^{18}O$ values in Figure 6. Note that although negative $\delta^{18}O$ carbonates are now possible this model still cannot generate the very lowest $\delta^{18}O$ value. In addition, the range of $\delta^{18}O$ values is limited to ~10‰ (not ~25‰ observed in the later stage cement) unless a large variation in H_2O:CO_2 from almost pure CO_2 to almost pure H_2O is invoked (Fig. 6).

4.3.2. Meteoric fluids

ALH84001 has well constrained formation age of 3.90 ± 0.04 Ga for the carbonate (Borg et al., 1999) and 3.92Ga ± 0.04 for maskelynite (Turner et al., 1997). Given the apparent scarcity of Ca-rich carbonate and interspersed maskelynite, it is reasonable to assume that age determinations are those of rosette carbonate and associated feldspathic material. There is no chronological data for the later stage cement, which could possibly be as young as the most recent hydrothermal events capable of causing secondary mineralisation i.e., a few hundred million years (Hartmann et al., 1999). In this type of environment, where the atmosphere is cold and CO_2 dominated, and H_2O is rare (like the present day is), Rayleigh distillation and CO_2 ice precipitation may be realistic.

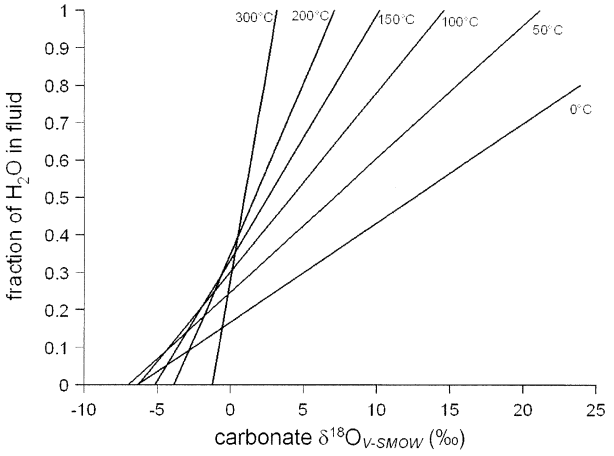

Fig. 6. In this model, isotherms are calculated with the assumption of high temperature equilibrium of CO_2 with pyroxene of $\delta^{18}O_{V\text{-}SMOW}$ +4.6‰ (fractionation factors from Bottinga and Javoy, 1975) followed by later precipitation from a lower temperature (0–300°C) H_2O/CO_2 fluid following the method of Clayton and Mayeda (1988). Oxygen equilibrium is attained in this lower temperature fluid between H_2O and CO_2 (fractionation factors from Friedman and O'Neil, 1977) but not between fluid and silicate. The isotopic composition of carbonate produced at a given temperature and H_2O:CO_2 ratio (plotted here as fraction O in H_2O) are displayed. Note that negative $\delta^{18}O$ carbonate can be produced but the isotopic variation is limited to ~10‰ unless H_2O:CO_2 changes greatly to more water rich compositions. This model also struggles to generate the very lowest $\delta^{18}O$ value.

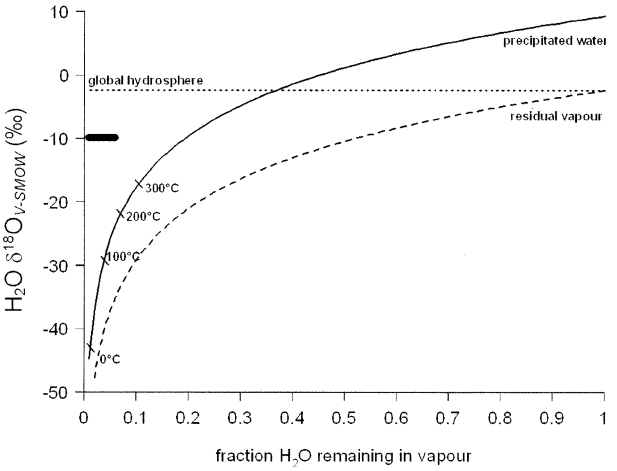

Fig. 7. Calculated isotopic compositions of water following Rayleigh fractionation of water vapour. Horizontal line for $\delta^{18}O = -2.4$‰ labelled global hydrosphere corresponds to a plausible isotopic composition for initial Martian water. Black bar is $\delta^{18}O_{V\text{-}SMOW}$ −10‰ Ca-rich carbonate. As Rayleigh fractionation proceeds Martian water evolves to progressively more negative $\delta^{18}O$ values. 0 to 300°C tick marks indicate the $\delta^{18}O$ of water that produces $\delta^{18}O_{V\text{-}SMOW}$ −10‰ carbonate at that temperature.

Although it is not clear what the atmospheric $\delta^{18}O$ of CO_2 could have been, particularly in view of evidence suggesting outgassing may have periodically altered the isotopic composition of the atmosphere (Farquhar and Thiemens, 2000), it is again assumed that the initial atmospheric has $\delta^{18}O_{CO2}$ of +43.7‰ and Rayleigh distillation fractionates this reservoir according to the CO_2 ice-vapour fractionation factor of Eiler et al. (2000). At plausible Martian atmospheric temperatures (160–180 K), Rayleigh distillation between CO_2 vapour and CO_2 ice, even assuming closed system fractionation to 99% completion, can generate CO_2 ice only 10‰ lower than the initial source fluid (i.e., with $\delta^{18}O_{CO2}$ ~ +34‰). Repeated evaporation and condensation episodes are required to generate lower $\delta^{18}O_{CO2}$ values. Although changes in obliquity may provide such a mechanism for cycling CO_2 (Mischna et al., 2003), the requirement of isolating this CO_2 from the global CO_2 reservoir over many evaporation/condensation cycles seems highly unlikely. Therefore production of meteoric CO_2 by simple Rayleigh fractionation of initial outgassed CO_2 is unlikely to be responsible for the isotopically light Ca-rich carbonate.

Although the composition, size and circulation of the early Martian atmosphere is not well constrained, many geological features strongly suggest a CO_2 dominated atmosphere of several bars which allowed liquid water at the surface. Early general circulation models calculated that Mars has cross-equatorial zonal circulation from 30°S to 30°N with two roughly symmetrical Earth-like Hadley-Ferrel cells (Haberle et al., 1993). Thus it may be possible that with zonal circulation cells, evaporation/condensation cycles permitted significant isotopic fraction of oxygen with latitude, in a manner similar to that on Earth (Antarctic ice can have $\delta^{18}O_{V\text{-}SMOW} = -50$‰). If we consider a similar Rayleigh fractionation process on Mars and again use an initial $\delta^{18}O_{H2O} = -2.4$‰ as suggested from planetary outgassing and cooling (Clayton and Mayeda, 1988) as our starting composition, we see that isotopic evolution of this water vapour would precipitate water with $\delta^{18}O_{V\text{-}SMOW}$ as low as −45‰ (Fig. 7). This can generate $\delta^{18}O_{V\text{-}SMOW} = -10$‰ carbonate at 0°C. This water is now capable of generating the whole range of $\delta^{18}O$ observed in the later stage cement if relatively small temperature fluctuations are invoked (Fig. 8). We also note that change of elevation with latitude is

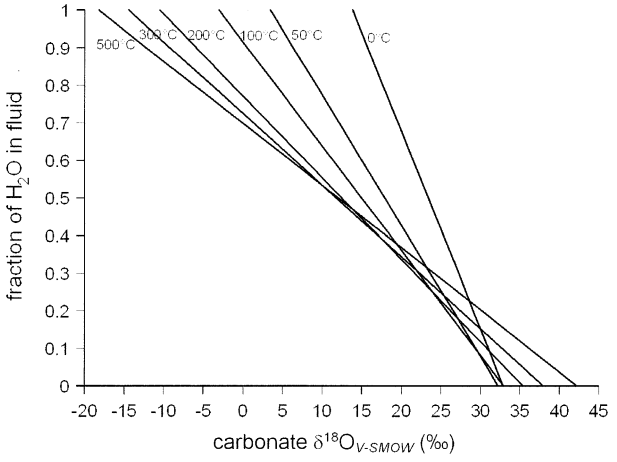

Fig. 8. Isotherms are calculated following the method of Clayton and Mayeda (1988) showing the isotopic composition of carbonate produced at a given temperature and H_2O:CO_2 ratio (displayed here as fraction O in H_2O). Initial composition of $CO_2 = \delta^{18}O_{V\text{-}SMOW}$ +43.7‰. This assumes H_2O:CO_2 = 0.8 after Clayton and Mayeda (1988) (see text). Initial composition of $H_2O = \delta^{18}O_{V\text{-}SMOW}$ −30‰ from Rayleigh fractionated water vapor (see Fig. 7). Mixing of these two components permits generation of carbonate with $\delta^{18}O_{V\text{-}SMOW}$ −10‰ at temperature as low as 150°C from a H_2O dominated fluid.

another mechanism by which atmospheric volatiles may be isotopically fractionated (e.g., Rowley et al., 2001) but this does not affect the arguments presented above. Indeed, given that the source region for ALH84001 is considered to be the ancient southern highlands, circulation of an air packet to a higher elevation may be a more feasible mechanism.

4.4. Relationship to Other SNC Carbonate

There is difficulty in generating all carbonate in ALH84001 (calcite with $\delta^{18}O = -10‰$ and magnesite with $\delta^{18}O = +24‰$) from a global reservoir of one isotopic composition: such a process requires dramatic variations in temperatures and/or fluid composition. If we require this universal reservoir to produce the heaviest observed carbonate of $\delta^{18}O = +34‰$ siderite in Nakhla (Saxton et al., 2000) this commonly used model is no longer capable of generating the observed $\delta^{18}O$ range of Martian carbonates. This ceases to be a problem if the $\delta^{18}O = -10‰$ carbonate was deposited from H_2O fractionated in the atmosphere, which is no longer representative of a global value. Equally, the hypothesis that secondary mineralisation in Nakhla is the product of an evaporative sequence (Bridges and Grady, 2000) also implies a fractionated local reservoir (in this case producing ^{18}O enriched fluids). Nevertheless, it is an important implication of our results that a hydrosphere reservoir of constant composition can no longer generate all carbonates observed in Martian meteorites over any range of temperatures. Either a locally produced ^{18}O depleted reservoir generated $\delta^{18}O_{V\text{-}SMOW} = -10‰$ carbonate and/or a locally produced ^{18}O enriched reservoir generated $\delta^{18}O_{V\text{-}SMOW} = +34‰$ siderite. If the later stage cement in ALH84001 were significantly older than Nakhla siderite, global evolution of O in the atmosphere could have occurred over time (Jakosky, 1993) generating both ALH84001 later stage cement with $\delta^{18}O_{V\text{-}SMOW} = -10‰$ and Nakhla carbonate with $\delta^{18}O_{V\text{-}SMOW} = +34‰$.

4.5. Implication for Ancient Mars

If the later stage cement was deposited from a water-rich fluid soon after the rosettes formed, it is possible that the substantial atmosphere inferred to permit precipitation of water may have been an early wet and warm atmosphere. However, it is also possible that the cement represents a significantly later influx of H_2O-CO_2 fluid. This is plausible given the evidence of water percolation in the nakhlites after their formation at 1.3 Ga (Bridges et al., 2001). If this were true, then the deposition event is likely to be volcanically induced. In this scenario, a hydrothermal episode could have remelted previously precipitated water ice with the light oxygen isotopic signature. This would not require an appreciable change in environment as the hydrothermal activity would likely to have been completely subsurface. Alternatively, volcanically induced outgassing may have resulted in a later substantial but transient atmosphere which precipitated water for a relatively short period of time. With igneous activity occurring until relatively recently (a few hundred million years) (Hartmann et al., 1999) and related flooding events capable of supplying more volatiles than the entire Martian atmosphere (McKenzie and Nimmo, 1999), this process appears feasible. Conceivably, the chaotic obliquity of Mars from 0 to 60° and the subsequent release of CO_2 and H_2O in both ices and clathrates may also be capable of generating a transient but substantial atmosphere (Jakosky et al., 1995; Mischna et al., 2003).

5. SUMMARY

We have documented evidence of previously unobserved carbonate textures containing isotopically light oxygen in carbonate. It appears that simple open system models are no longer capable of explaining the range of $\delta^{18}O$ values found in ALH84001. The well understood terrestrial process of atmospheric water precipitation has been proposed as a mechanism for producing sufficiently ^{18}O depleted water on Mars. Given the apparently unique nature of these samples, it is unlikely that dating of ALH84001 carbonate represents the age of carbonate presented here. Should meteoric water be the source, an age of ~4 Ga may be compatible with a wet/warm early Mars whereas a substantially younger age would imply a temporary but substantial atmosphere on Mars or remelting of previously fractionated subsurface water ice.

Acknowledgments—We are grateful to the Particle Physics and Astronomy Research Council (PPARC) for support for this work for JMS and a studentship for GH. We are indebted to K. McKeegan and C. Coath for the opportunity to obtain oxygen isotope ratio measurements of these samples using the UCLA Cameca 1270 ion probe and permission to publish this data. We thank D. Plant for assistance with EPMA analyses, D. J. Blagburn and B. Clementson for technical support and NASA for provision of samples through its Ancient Mars Meteorite Program. We thank Jamie Gilmour for constructive comments on early versions of this manuscript. Finally, we thank three anonymous reviewers for constructive comments and M. Grady for additional help.

Associate editor: M. M. Grady

REFERENCES

Borg L. E., Connelly J. N., Nyquist L. E., Shih C. Y., Wiesmann H., and Reese Y. (1999) The age of the carbonates in Martian meteorite ALH84001. *Science* **286,** 90–94.

Bottinga Y. and Javoy M. (1975) Oxygen isotope partitioning among the minerals in igneous and metamorphic rocks. *Rev. Geophys. Space Phys.* **13,** 401–418.

Brearley A. J. (1998) Rare K-bearing mica in ALH 84001: Additional constraints on carbonate formation. *Lunar Planet. Inst. Contrib. Workshop Martian Meteorit* **956,** 6–8.

Brearley A. J. (2000) Hydrous phases in ALH84001: Further evidence for preterrestrial alteration and a shock-induced thermal overprint. *Proc. 31st Lunar Planet. Sci. Conf.*, abstract #1203.

Bridges J. C., Catling D. C., Saxton J. M., Swindle T. D., Lyon I. C., and Grady M. M. (2001) Alteration assemblages in Martian meteorites: Implications for near-surface processes. In *Chronology and Evolution of Mars* (eds. R. Gallenbach, J. Geiss, and W. K. Hartmann), **96,** pp. 365–392. Kluwer Academic Publishers, Amsterdam, the Netherlands.

Bridges J. C. and Grady M. M. (2000) Evaporite mineral assemblages in the nakhlite (Martian) meteorites. *Earth Planet. Sci. Lett.* **176,** 267–279.

Chiba H., Chacko T., Clayton R. N., and Goldsmith J. R. (1989) Oxygen isotope fractionations involving diopside, forsterite, magnetite and calcite: Applications to geothermometry. *Geochim. Cosmochim. Acta* **53,** 2985–2995.

Clayton R. N. and Mayeda T. K. (1988) Isotopic composition of carbonate EETA 79001 and its relation to parent body volatiles. *Geochim. Cosmochim. Acta* **52,** 925–927.

Clayton R. N. and Mayeda T. K. (1996) Oxygen isotope studies of achondrites. *Geochim. Cosmochim. Acta* **60,** 1999–2017.

Corrigan C. M. and Harvey R. P. (2004) Multi-generational assemblages in Martian meteorite Allan Hills 84001: Implications for nucleation, growth and alteration. *Meteorit. Planet. Sci*. **39,** 17–30.

Eiler J. M., Kitchen N., and Rahn T. A. (2000) Experimental constraints on the stable-isotope systematics of CO_2 ice/vapor systems and relevance to the study of Mars. *Geochim. Cosmochim. Acta* **64,** 733–746.

Eiler J. M., Valley J. W., Graham C. M., and Fournelle J. (2002) Two populations of carbonate in ALH84001: Geochemical evidence for discrimination and genesis. *Geochim. Cosmochim. Acta* **66,** 1285–1303.

Farquhar J. and Thiemens M. H. (2000) Oxygen cycle of the Martian atmosphere-regolith system: $\Delta^{17}O$ of secondary phases in Nakhla and Lafayette. *J. Geophys. Res*. **105,** 11991–11997.

Farquhar J., Thiemens M. H., and Jackson T. (1998) Atmosphere-surface interactions on Mars: $\Delta^{17}O$ measurements of carbonate from ALH 84001. *Science* **280,** 1580–1582.

Franchi I. A., Wright I. P., Sexton A. S., and Pillinger C. T. (1999) The oxygen-isotopic composition of Earth and Mars. *Meteorit. Planet. Sci*. **34,** 657–661.

Friedman I. and O'Neil J. R. (1977) Data of geochemistry. Compilation of stable isotope fractionation factors of geochemical interest. *Geol. Surv. Prof. Paper 440-KK*. 6th ed.

Golden D. C., Ming D. W., Schwandt C. S., Morris R. V., Yang S. V., and Lofgren G. E. (2000) An experimental study on kinetically-driven precipitation of calcium-magnesium-iron carbonates from solution: Implications for the low-temperature formation of carbonates in Martian meteorite Allan Hills 84001. *Meteorit. Planet. Sci* **35,** 457–465.

Haberle R. M., Pollack J. B., Barnes J. R., Zurek R. W., Leovy C. B., Murphy J. R., Lee H., and Schaeffer J. (1993) Mars atmospheric dynamics as simulated by the NASA AMES general circulation model 1. The zonal mean circulation. *J. Geophys. Res* **98,** 3093–3123.

Hartmann W. K., Malin M., McEwen A., Carr M., Soderbolm L., Thomas P., Danielson E., James P., and Veverka J. (1999) Evidence for recent volcanism on Mars from crater counts. *Nature* **397,** 586–589.

Harvey R. P. and McSween H. Y., Jr. (1996) A possible high-temperature origin for the carbonates in Martian meteorite ALH84001. *Nature* **382,** 49–51.

Harvey R. P. and McSween H. Y., Jr. (1998) An evaporation model for formation of carbonates in the ALH84001 Martian meteorite. *Int. Geol. Rev*. **40,** 774–783.

Jakosky B. M. (1993) Mars volatile evolution: Implications of the recent measurement of ^{17}O in water from the SNC meteorites. *Geophys. Res. Lett* **20,** 1591–1594.

Jakosky B. M., Henderson B. G., and Mellon M. T. (1995) Chaotic obliquity and the nature of the Martian climate. *J. Geophys. Res*. **100,** 1579–1584.

Jones R. H., Saxton J. M., Lyon I. C., and Turner G. (2000) Oxygen isotopes in chondrule olivine and isolated olivine grains from the CO3 chondrite Allan Hills A77307. *Meteorit. Planet. Sci*. **35,** 849–857.

Jull A. J. T., Eastoe C. J., Xue S., and Herzog G. F. (1995) Isotopic composition of carbonate in the SNC meteorites Allan Hills 84001 and Nakhla. *Meteoritics* **30,** 311–318.

Karlsson H. R., Clayton R. N., Gibson E. K., Jr., and Mayeda T. K. (1992) Water in SNC meteorites: Evidence for a Martian hydrosphere. *Science* **255,** 1409–1411.

Kent A. J. R., Hutcheon I. D., Ryerson F. J., and Phinney D. L. (2001) The temperature of formation of carbonate in Martian meteorite ALH84001: Constraints from cation diffusion. *Geochim. Cosmochim. Acta* **65,** 311–321.

Krasnopolsky V. A., Mumma M. J., Bjoraker G. L., and Jennings D. E. (1996) Oxygen and carbon isotope ratios in Martian carbon dioxide: Measurements and implications for atmospheric evolution. *Icarus* **124,** 553–568.

Leshin L. A., McKeegan K. D., Carpenter P. K., and Harvey R. P. (1998) Oxygen isotopic constraints on the genesis of carbonates from Martian meteorite ALH 84001. *Geochim. Cosmochim. Acta* **62,** 3–13.

Martinez I., Agrinier P., Schärer U., and Javoy M. (1994) A SEM-ATEM and stable isotope study of carbonates from the Haughton impact crater, Canada. *Earth Planet. Sci. Lett*. **121,** 559–574.

McKay D. S., Gibson E. K., Jr., Thomas-Keptra K. L., Vali H., Romanek C. S., Clemett S. J., Chillier X. D. F., Maechling C. R., and Zare R. N. (1996) Search for past life on Mars: Possible relic biogenic activity in Martian Meteorite ALH84001. *Science* **273,** 924–930.

McKenzie D. and Nimmo F. (1999) The generation of Martian floods by the melting of ground ice above dykes. *Nature* **397,** 231–233.

Mischna M. A., Richardson M. I., Wilson J. R., and McCleese D. J. (2003) On the orbital forcing of Martian water and CO_2 cycles: A general circulation model study with simplified volatiles schemes. *J. Geophys. Res*. **108,** 16–25.

Mittlefehldt D. W. (1994) ALH84001, a cumulate orthopyroxenite member of the Martian meteorite clan. *Meteoritics*. **29,** 214–221.

Nier A. O. and McElroy M. B. (1977) Composition and structure of Mars' upper atmosphere: Results from the neutral mass spectrometers on Viking 1 and 2. *J. Geophys. Res*. **82,** 4341–4349.

Nyquist L. E., Bansal B. M., Wiesmann H., and Shih C.-Y. (1995) "Martians" young and old: Zagami and ALH84001[abstract]. *Lunar Planet. Sci*. **26,** 1065–1066.

Romanek C. S., Grady M. M., Wright I. P., Mittlefehldt D. W., Socki R. A., Pillinger C. T., and Gibson E. K., Jr. (1994) Record of fluid-rock interactions on Mars from the meteorite ALH84001. *Nature*. **372,** 655–657.

Rowley D. B., Pierrehumbert R. T., and Currie B. S. (2001) A new approach to stable isotope-based paleoaltimetry: Implications for paleoaltimetry and paleohypsometry of the High Himalaya since the Late Miocene. *Earth. Planet. Sci. Lett*. **188,** 253–268.

Saxton J. M., Lyon I. C., Chatzitheodoridis E., Perera I. K., van Lierde P., Freedman P., and Turner G. (1996) The Manchester Isolab 54 ion microprobe. *Int. J. Mass Spec. Ion Proc*. **154,** 99–131.

Saxton J. M., Lyon I. C., and Turner G. (1998) Correlated chemical and isotopic zoning in carbonates in Martian meteorites ALH84001. *Earth Planet. Sci. Lett*. **160,** 811–822.

Saxton J. M., Lyon I. C., Chatzitheodoridis E., and Turner G. (2000) Oxygen isotopic composition of carbonate in the Nakhla meteorite: Implications for the hydrosphere and atmosphere of Mars. *Geochim. Cosmochim. Acta*. **64,** 1299–1309.

Scott E. R. D. (1999) Origin of carbonate-magnetite-sulfide assemblages in Martian meteorite ALH84001. *J. Geophys. Res*. **104,** 3803–3813.

Scott E. R. D., Yamaguchi A., and Krot A. N. (1997) Petrological evidence for shock melting of carbonates in the Martian meteorite Allan Hills 84001. *Nature*. **387,** 377–379.

Scott E. R. D., Krot A. N., and Yamaguchi A. (1998) Carbonates in fractures of Martian meteorite ALH84001: Petrologic evidence for impact origin. *Meteorit. Planet. Sci*. **33,** 709–719.

Shearer C. K., Leshin L. A., and Adcock C. T. (1999) Olivine in Martian meteorite Allan Hills 84001: Evidence for a high-temperature origin and implications for signs of life. *Meteorit. Planet. Sci*. **34,** 331–339.

Skála R. and Žák K. (2001) Stable isotope study of carbonates from the Ries meteorite crater—Evidence for impact induced carbonate decomposition. *Lunar Planet. Sci*. **32,** Abstract #1572.

Treiman A. H. (1995) A petrographic history of Martian meteorite ALH 84001: Two shocks and an ancient age. *Meteoritics*. **30,** 294–302.

Treiman A. H. (1998) The history of Allan Hills 84001 revised: Multiple shock events. *Meteorit. Planet. Sci*. **33,** 753–764.

Treiman A. H. and Romanek C. S. (1998) Bulk and stable isotopic compositions of carbonate minerals in the Martian meteorite Allan Hills 84001: No proof of high formation temperature. *Meteorit. Planet. Sci*. **33,** 737–742.

Turner G., Knott S. F., Ash R. D., and Gilmour J. D. (1997) Ar-Ar chronology of the Martian meteorite ALH84001: Evidence for the timing of the early bombardment of Mars. *Geochim. Cosmochim. Acta*. **61,** 3835–3850.

Valley J. W., Eiler J. M., Graham C. M., Gibson E. K., Jr., Romanek C. S., and Stolper E. M. (1997) Low-temperature carbonate concretions in the Martian meteorites ALH84001: Evidence from stable isotopes and mineralogy. *Science*. **275,** 1633–1638.

Warren P. H. (1998) Petrologic evidence for low-temperature, possibly flood evaporitic origin of carbonates in the ALH84001 meteorite. *J. Geophys. Res.* **103,** 16759–16773.

Wright I. P., Grady M. M., and Pillinger C. T. (1992) Chassigny and the nakhlites: Carbon-bearing components and their relationship to Martian environmental conditions. *Geochim. Cosmochim. Acta.* **56,** 817–826.

APPENDIX

SUPPLEMENTARY DATA

Supplementary data associated with this article can be found, in the online version, at doi:10.1016/j.gca.2004.08.023.